ELSEVIER

Chemical Engineering Journal 84 (2001) 193–200

Chemical Engineering Journal

www.elsevier.com/locate/cej

Gas-assisted displacement of a Newtonian fluid confined in a Hele-Shaw cell

Fethi Kamişli*, Michael E. Ryan

Department of Chemical Engineering, State University of New York at Buffalo, Amherst, NY 14260, USA

Received 9 December 1998; received in revised form 26 April 2000; accepted 25 September 2000

Abstract

The two-dimensional flow in a rectangular channel containing a Newtonian fluid was solved analytically in terms of eigenfunctions as $\theta \rightarrow \pi/2$, where θ is the angle between the normal to the interface and the axial direction. From this analysis, the relationship between the parameters C_a, λ, and kd were obtained. These parameters are related to the amount of liquid deposited on the walls of the rectangular channel. This analysis provides a satisfactory relationship between m and C_a for values of kd between 1.8 and 2.0. It is expected that the coating thickness obtained from this analysis for a rectangular channel is close to the experimental data for a value of kd taken to be 1.95 since the perturbation solution at low capillary number is close to this value of kd. The solution is valid for an interface is almost parallel to the walls of the Hele-Shaw cell.

Keywords: Newtonian fluid; Hele-Shaw cell; Gas-assisted displacement

1. Introduction

The motion of long bubbles into Newtonian fluids confined in horizontal cylindrical tubes or channels of rectangular cross-section (Hele-Shaw cell) has been studied for several years. When a less viscous fluid displaces a more viscous fluid from the gap between two closely spaced parallel plates, the interface develops a tongue-like shape with the less viscous fluid penetrating into the more viscous fluid. Similarly, when air is forced into one end of a circular tube containing a viscous liquid, it forms a round-ended column or bullet-like shape which travels down the tube forcing some liquid out at the far end and leaving a fraction of the liquid m, in the form of an annular layer covering the wall. In the case of a square channel the shape of the less viscous fluid penetrating into the more viscous fluid depends on the velocity of the less viscous fluid. If the velocity of the less viscous fluid (called the bubble or finger hereafter) is larger than a certain limiting value, the bubble assumes a bullet-like shape; otherwise, the bubble conforms to the shape of the square channel. In a rectangular channel, if the capillary number, $C_a = \mu u_b/\sigma$, is not too large, a single steady-state tongue-like shape moves through the cell with constant velocity u_b, where μ is the viscosity of the driven liquid, u_b the bubble velocity, and σ the gas–liquid interfacial tension. In a circular tube or square channel, the bullet-like shape of the bubble persists even at very large capillary number. In other words, the fingering effect does not occur in the case of a long bubble advancing in either a circular tube or a square channel at large capillary numbers.

Most analytical and/or numerical studies of gas-assisted displacement in rectangular channels, and other geometries, commonly assume that the flow is two-dimensional. The fact that the gap thickness between the two planes, denoted as $2d$, is very small makes it possible to derive the two-dimensional flow field equations.

As mentioned previously, gas-assisted liquid displacement, has been extensively investigated for more than 60 years. Fairbrother and Stubbs [14] performed the first experiments to determine the amount of liquid left inside of a tube when it is displaced by another immiscible fluid. They determined the flow rate of the liquid by measuring the motion of the gas interface in the tube. An empirical correlation for the fraction of the liquid deposited on the walls of the tube was formulated as follows:

$$m = \frac{u_b - u}{u_b} = 1.0C_a^{1/2} = \left(\frac{\mu u_b}{\sigma}\right)^{1/2}$$

This result was found satisfactory for capillary numbers between 10^{-3} and 10^{-2}.

* Corresponding author. Present address: Department of Chemical Engineering, Faculty of Engineering, Firat University, 23279 Elazığ, Turkey.
E-mail address: fkamisli@firat.edu.tr (F. Kamişli).

1385-8947/01/$ – see front matter
PII: S1385-8947(00)00275-8

Isothermal gas-assisted displacement of Newtonian liquids in circular tubes was also experimentally studied by Taylor [4]. By plotting the fraction of the liquid as a function of the capillary number, he collapsed the data on to a single curve, and showed that this fraction asymptotically approached the value of 0.56 for a capillary number nearly equal to 2. Cox [1,2] extended Taylor's [4] result to capillary numbers up to 10 and showed that the limiting fraction of the liquid deposited on the walls of the tube was approximately 0.6. His theoretical analysis resulted in a fourth-order differential equation in terms of the stream function. Inertial and gravitational forces were neglected. The streamlines were assumed to be a specific function of the spatial coordinates. The governing equations were expressed in matrix form and solved numerically.

Bretherton [3] also undertook a theoretical analysis of this problem for circular capillaries. He found an approximate solution using the method of matched asymptotic expansions. The idea behind this theoretical treatment is that for sufficiently small C_a the viscous stresses appreciably modify the static profile of the bubble only very near to the wall. In this region, the lubrication approximation gives a good description of the flow field and of the interface profile. In the center of the capillary, the static profile is valid and there is a region of overlap in which the two solutions are matched. Using the lubrication approximation which requires quasi-unidirectional flow in the thin liquid film and assuming the slope of the fluid–fluid interface to be small, it can be shown that the velocity profile is parabolic. The boundary conditions for steady flow are the no-slip condition at the capillary wall, and tangential stress equal to zero at the fluid interface. The bubble is assumed to be inviscid resulting in a constant pressure within the bubble. The pressure in the liquid film is given by the pressure drop across the interface which is approximated by the Young–Laplace equation. Bretherton [3] also systematically explored a number of possible causes for the discrepancy between the analysis and experimental data. Schwartz et al. [15] considered the same problem and found some differences in liquid film thickness for sufficiently long bubbles, as compared to short bubbles.

An experimental study by Marchessault and Mason [19] used air bubbles in a dilute aqueous solution of potassium chloride. Film thicknesses were inferred from resistance measurements and were found to be substantially larger than those reported by Bretherton [3]. The residual wetting layer of the displaced liquid will vary with the velocity of advance of the interface.

Numerical studies of capillary tube displacement of a wetting liquid by a semi-infinite inviscid slug of gas have been presented. Both Reinelt and Saffman [9] using a finite difference method and Shen and Udell [20] using a finite element approach solved the full creeping-motion equations with the continuity of stress imposed exactly on the free surface.

Ratulowski and Chan [6] investigated a single discrete bubble and the motion of a long bubble in a circular tube and square channel. They determined the fraction of liquid deposited on the walls of the tube or channel and the pressure drop across the bubble front. According to their study, a single isolated bubble resembles an infinitely long bubble in terms of determining the film thickness and pressure drop across the bubble front if the length of the bubble exceeds the channel width. Their analysis is only valid for $C_a > 3 \times 10^{-3}$.

Kolb and Cerro [11] studied the isothermal gas-assisted displacement of a Newtonian liquid from a channel of square cross-section and showed that the liquid deposited on the wall of the square tube also approaches an asymptotic limit at high capillary numbers. Above $C_a = 0.1$, the gas forms a circular hollow core and thicker liquid deposition; below $C_a = 0.1$ the hollow core takes on the square cross-section of the tube as the deposition thickness is reduced. The above study was extended [10] by adding the lubrication approximation for intermediate to large capillary numbers where the flow is axisymmetric. In their work the film thickness on the walls of the square channel can be predicted as a function of capillary number since the velocity profile of the fluid flowing between the bubble and the square channel walls is known. It was claimed that the lubrication approximation solution is in good agreement with experimental data for values of capillary number between 0.7 and 2.0.

Unlike previous investigators, Poslinski et al. [21] investigated non-Newtonian fluids deposited on the walls of a tube. They found that the fraction of the non-Newtonian fluid deposited on the walls is less than that of a corresponding Newtonian fluid at low capillary number. At higher capillary number the fraction of the liquid deposited asymptotically increases and approaches a value of 0.58.

Poslinski and Coyle [22] have also examined shear thinning effects using numerical simulation of the gas-assisted displacement of non-Newtonian fluids in a tube and slit. Numerical results indicated that fluids with a shear thinning viscosity exhibit a thinner liquid film thickness than corresponding Newtonian fluids.

Huzyak and Koelling [25] experimentally investigated the gas-assisted displacement of non-Newtonian fluids deposited on the walls of a tube. They examined the effect of fluid elasticity and tube diameter on the fractional coverage. Their study showed that unlike Newtonian fluids, the fractional coverage for viscoelastic fluid did not reach an asymptotic value but continued to increase, attaining a value in excess of 0.73, and that the fractional coverage of viscoelastic fluids decreases with increasing tube diameter.

Ro and Homsy [17] performed an asymptotic analysis of the gas-assisted displacement of a non-Newtonian fluid in a Hele-Shaw cell. The effects of normal stress and shear stress thinning in determining the film thickness and the pressure jump across the interface were examined. Viscoelastic fluids were modeled by an Oldroyd-B constitutive equation and the solutions for the constant film thickness region and the static meniscus region were matched in the transition regime as for the Newtonian case [5].

The planar geometry or Hele-Shaw cell consists of two closely separated parallel plates having a distance $2d$ between them. The sides of this rectangular channel are at a distance $2Z_0$ apart where $d \ll Z_0$. A parameter λ is defined as (thickness of gas bubble)/(distance between the plates). In the rectangular channel the thickness of the tongue-like shape is $2\lambda d$ and its width is $2\lambda_w Z_0$, where the parameter λ_w is equal to (width of the bubble)/(width of the rectangular channel).

The determination of the value of λ and λ_w has been a subject of much interest. The determination of λ_w as a function of capillary number, C_a, for different cell aspect ratios, Z_0/d, has been examined experimentally by Saffman and Taylor [24], Pitts [18], and Tabeling et al. [23]. Saffman and Taylor [24] and Pitts [18] found that the value of λ_w decreases monotonically to 0.5 when the bubble velocity is increased. In contrast, Tabeling et al. [23] reported that the value of λ_w never decreases to 0.5 when the bubble velocity is increased. The problem was reconsidered by McLean and Saffman [16] by including surface tension effects due to the lateral curvature of the interface of the advancing finger. In their numerical study the value of λ_w was close to 0.5 at large bubble velocity which is in good agreement with the experimental data. At low velocities (i.e. $C_b = 12C_a(Z_0/d)^2 < 100$), the agreement with experiment was ambiguous since the finger sizes predicted by the theory were significantly below those actually measured. They found that the incorporation of surface tension and cell aspect ratio did not remedy or reduce the disagreement between theory and experiment in terms of calculating the value of λ_w as a function of C_b.

The approach of Bretherton [3] was reconsidered by Park and Homsy [5] in the horizontal Hele-Shaw cell at very low capillary number. The problem was solved using a perturbation method with an asymptotic expansion of $C_a^{1/3}$ and the ratio of the gap width to the transverse characteristic length $\delta_e = d/Z_0$ as small quantities. They obtained relationships between λ, C_a, and δ_e for calculating the film thickness and pressure jump across the bubble front. The resulting expressions were compared with the results of Bretherton [3] and Landau and Levich [13] were considered to give improved results.

Reinelt [8] extended his earlier work by determining the perturbation solution of the axisymmetric flow problem for small values of C_a and $\delta = d/R$. In his study, some of the boundary conditions were improved by incorporating the film thickness into the kinematic boundary condition and taking into account the dependence of Δp on the capillary number. The problem was also numerically solved using a conformal mapping method and the numerical results were presented in another paper [7]. Although the inclusion of the effects of the film thickness variation and the lateral and transverse curvature on the interface boundary conditions improved the quantitative agreement between the experimental and numerical results, it did not remove the discrepancy associated with different finger widths.

In this paper, the two-dimensional flow in a rectangular channel containing a Newtonian fluid was solved analytically in terms of eigenfunctions as $\theta \to \pi/2$, where θ is the angle between the normal to the interface and the axial direction. From this analysis, the relationship between the parameters C_a, λ, and kd were obtained. These parameters are related to the amount of liquid deposited on the walls of the rectangular channel. The procedure followed was similar to that of Cox [1]. This analysis differs from Cox's analysis in terms of the geometry considered.

2. General formulation

When a less viscous fluid displaces a more viscous fluid from a rectangular channel two closely spaced parallel plates, interface develops a tongue-like shape with the less viscous fluid penetrating into the more viscous fluid.

Consider the motion of a gas bubble in an incompressible Newtonian liquid in a rectangular channel as shown in Fig. 1. The planar geometry consists of two closely separated parallel plates having a perpendicular distance $2d$ between them. For the case of displacement between two flat, parallel, horizontal plates, since $d \ll Z_0$, a two-dimensional approximation to the flow is valid. The equations of continuity and motion for an incompressible Newtonian or non-Newtonian fluid are given by

$$\frac{1}{\dot{y}^a}\frac{\partial}{\partial \dot{y}}(\dot{y}^a \dot{u}) + \frac{\partial \dot{v}}{\partial \dot{x}} = 0 \tag{1}$$

$$\rho\left(\frac{\partial \dot{v}}{\partial \dot{t}} + \dot{v}\frac{\partial \dot{v}}{\partial \dot{x}} + \dot{u}\frac{\partial \dot{v}}{\partial \dot{y}}\right) = -\frac{\partial \dot{p}}{\partial \dot{x}} - \left[\frac{1}{\dot{y}^a}\frac{\partial}{\partial \dot{y}}(\dot{y}^a \tau_{yx}) + \frac{\partial \tau_{xx}}{\partial \dot{x}}\right] \tag{2}$$

$$\rho\left(\frac{\partial \dot{u}}{\partial \dot{t}} + \dot{v}\frac{\partial \dot{u}}{\partial \dot{x}} + \dot{u}\frac{\partial \dot{u}}{\partial \dot{y}}\right) = -\frac{\partial \dot{p}}{\partial \dot{y}} - \left[\frac{1}{\dot{y}^a}\frac{\partial}{\partial \dot{y}}(\dot{y}^a \tau_{yy}) + \frac{\partial \tau_{yx}}{\partial \dot{x}}\right] \tag{3}$$

The parameter a has a value of either 0 or 1 depending on the geometry (0 corresponds to the planar case and 1 corresponds to a cylindrical geometry). τ_{ij} is the stress tensor

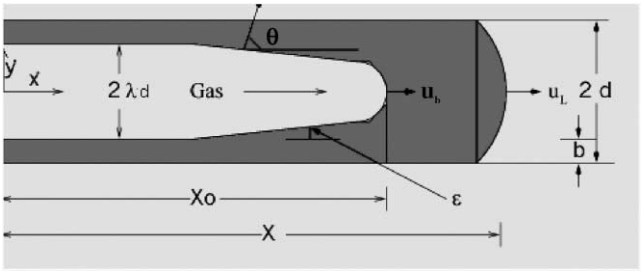

Fig. 1. Schematic diagram of gas-assisted displacement.

and $\dot{p}$ the pressure. The velocity components $\dot{v}$ and $\dot{u}$ are in the $\dot{x}$ and $\dot{y}$ directions, respectively. The $\dot{y}$-axis is taken normal to the channel plates (or tube wall) with the origin at the mid-plane (or tube axis). Thus $\dot{y}$ has the value of $\pm d$ for the planar case at the solid boundaries. The appropriate solution requires that the boundary conditions must be applied on the walls of the channel and along the free surface. In this investigation, no-slip conditions are applied at the solid boundaries. In order to find the appropriate interface boundary condition, the viscosity of the gas within the bubble is neglected when compared with the viscosity of the fluid exterior to the bubble. The tangential stress boundary condition at the interface is given by

$$\tau_{yy} n_y t_y + \tau_{xy} n_x t_y + \tau_{yx} n_y t_x + \tau_{xx} n_x t_x = 0 \tag{4}$$

where n_i and t_i are the components of **n** and **t** which are unit vectors normal and tangent to the interface, respectively.

The difference in the normal stress on the two sides of the interface is balanced by the surface tension and is expressed as

$$\tau_{yy} n_y^2 + \tau_{xx} n_x^2 + 2\tau_{xy} n_x n_y = -p_0 + \frac{\sigma}{\dot{R}} \tag{5}$$

where $\dot{R}$ is the principal radius of curvature of the interface, σ the interfacial tension, and p_0 the pressure within the gas bubble. τ_{ij} is the total stress and is defined as

$$\tau_{ij} = -\dot{p}\delta_{ij} + \mu\left(\frac{\partial \dot{v}_i}{\partial \dot{x}_j} + \frac{\partial \dot{v}_j}{\partial \dot{x}_i}\right)$$

where

$$\delta_{ij} = \begin{cases} 0 & \text{if} \quad i \neq j, \\ 1 & \text{if} \quad i = j \end{cases}$$

3. Analytical solution for Newtonian fluid in a rectangular channel

In this analysis, it is assumed that the velocity of the liquid varies not only in the axial direction but also in the transverse direction. The frame of reference is taken with respect to the stationary walls of the rectangular channel and the problem is solved as $\theta \to \pi/2$, where θ is the angle between the normal to the interface and the axial direction. It is assumed that the long gas bubble is moving into the viscous fluid at a constant velocity in the positive x-direction. On the solid boundaries the no-slip condition is applied. In order to develop the appropriate interface conditions, the viscosity of the gas within the bubble is neglected when compared with the viscosity of the fluid exterior to the bubble. For convenience, velocities are nondimensionalized by the uniform bubble velocity u_b, the transverse and axial coordinates by the characteristic length d, and the pressure by σ/d. The characteristic length d is taken to be the half distance between the parallel plates. The dimensionless variables are defined as follows:

$$x = \frac{\dot{x} - u_b t}{d}, \qquad y = \frac{\dot{y}}{d}, \qquad R = \frac{\dot{R}}{d},$$
$$v = \frac{\dot{v}}{u_b}, \qquad u = \frac{\dot{u}}{u_b}, \qquad p = \frac{\dot{p}}{\sigma/d}$$

It is also assumed that in this approach the inertia terms are negligible when compared with the viscous terms. In other words, the Reynolds number is much less than unity ($Re = \rho u_b d/\mu \ll 1$). Thus, Eqs. (1)–(3) for this two-dimensional flow ($a = 0$) become

$$\frac{\partial v}{\partial x} + \frac{\partial u}{\partial y} = 0 \tag{6}$$

$$\frac{\partial p}{\partial x} = C_a\left[\frac{\partial^2 v}{\partial x^2} + \frac{\partial^2 v}{\partial y^2}\right] \tag{7}$$

$$\frac{\partial p}{\partial y} = C_a\left[\frac{\partial^2 u}{\partial x^2} + \frac{\partial^2 u}{\partial y^2}\right] \tag{8}$$

where the capillary number C_a is the ratio of the viscous force to the force due to surface tension. After eliminating pressure from the above equations and introducing the stream function into the resulted equation gives

$$\left(\frac{\partial^2}{\partial x^2} + \frac{\partial^2}{\partial y^2}\right)^2 \psi(x, y) = 0 \tag{9}$$

The stream function is given by

$$v = \frac{\partial \psi}{\partial y}, \qquad u = -\frac{\partial \psi}{\partial x}$$

For the chosen frame of reference, the boundary conditions are expressed as follows. The tangential and normal components of velocity of the liquid at the walls of the channel are zero. Therefore

$$\frac{\partial \psi}{\partial y} = \frac{\partial \psi}{\partial x} = 0 \quad \text{at} \quad y = \pm d \tag{10}$$

The kinematic boundary condition at the interface is given by

$$(v - 1)n_x + u n_y = 0 \tag{11}$$

According to the specified frame of reference n_x and n_y are given by $n_x = \cos\theta$, $n_y = \sin\theta$ and the relationships between the unit normal and tangent vectors are $t_y = -n_y$ and $t_x = n_y$.

Substituting the stress tensor into Eqs. (4) and (5) gives the tangential stress and normal stress boundary conditions at the interface

$$2\left(\frac{\partial v}{\partial x}\right) t_x n_x + (t_x n_y + t_y n_x)\left(\frac{\partial v}{\partial y} + \frac{\partial u}{\partial x}\right) + 2\left(\frac{\partial u}{\partial y}\right) n_y t_y = 0 \tag{12}$$

$$-p(n_x^2+n_y^2)+2C_a \times\left[\left(\frac{\partial u}{\partial y}\right)n_y^2+\left(\frac{\partial v}{\partial x}\right)n_y^2+\left(\frac{\partial v}{\partial y}+\frac{\partial u}{\partial x}\right)n_y n_x\right] = -p_0+\frac{1}{R} \quad (13)$$

Eqs. (11)–(13) are the three interfacial boundary conditions, namely the kinematic, tangential and normal stress boundary conditions that must be satisfied by the solution.

Since when a less viscous fluid displaces a more viscous fluid from the gap between two closely spaced parallel plates, an interface develops a tongue-like shape with the less viscous fluid, the interface profile can be expressed in terms of an exponential dependence on x as $\theta \to \pi/2$. In other words, the stream function at the interface can be taken to be of the form $\psi(x, y) = \varpi(y)\exp(kx)$. This will give a relationship between k, decay rate, λ, and C_a. As $\theta \to \pi/2$, $\varepsilon \to 0$ as shown in Fig. 1. Therefore, this form of the stream function is valid and ε has identical form as the stream function, namely $\varepsilon = \varepsilon_0 \exp(kx)$ for small ε_0 [1], where ε is the distance from the constant film thickness position to the interface as $\theta \to \pi/2$. The radius of the long gas bubble can be taken to be equal to $r = \lambda d - \varepsilon$ for some small positive perturbation.

The assumption of small ε implies that the analysis is valid when the interface is almost parallel to the walls of the tube or channel. Substituting the assumed form of the stream function into Eq. (9) gives

$$\left(\frac{\partial^2}{\partial y^2}+k^2\right)^2 \varpi(y) = 0 \quad (14)$$

The solution of Eq. (14) and the relationship between ϖ and ψ give

$$\psi(x, y) = \left\{A\left(\frac{y}{2k}\sin ky+\frac{1}{4k^2}\sin 2ky\sin ky+\frac{1}{4k^2}\cos 2ky\cos ky\right) +B\left(-\frac{y}{2k}\cos ky-\frac{1}{4k^2}\sin ky\cos 2ky+\frac{1}{4k^2}\sin 2ky\cos ky\right) +C\cos ky+D\sin ky\right\}\exp(x, y) \quad (15)$$

Here A, B, C, and D are arbitrary constants. In order to obtain the pressure for the viscous fluid in the axial direction, Eq. (7) is expressed in terms of the stream function and combined with Eq. (15). After some manipulation, the resulting equation is

$$p = C_a(-A\sin ky + B\sin ky)\exp(ky) + F \quad (16)$$

where F is a constant. All of the boundary conditions can be re-expressed in terms of the stream function (Eq. (15)) as follows.

The axial velocity at the walls of the channel is

$$A\left(\frac{1}{2k}\sin kd+\frac{d}{2}\cos kd+\frac{1}{4k}\cos 2kd\sin kd -\frac{1}{4k}\sin 2kd\cos kd\right)+B\left(-\frac{1}{2k}\cos kd+\frac{d}{2}\sin kd +\frac{1}{4k}\sin 2kd\sin kd+\frac{1}{4k}\cos 2kd\cos kd\right) -kC\sin kd+kD\cos kd = 0 \quad (17)$$

Transverse velocity at the walls of the channel is

$$A\left(\frac{d}{2}\sin kd+\frac{1}{4k}\sin 2kd\sin kd+\frac{1}{4k}\cos 2kd\cos kd\right) +B\left(-\frac{d}{2}\cos kd-\frac{1}{4k}\cos 2kd\sin kd+\frac{1}{4k}\sin 2kd\cos kd\right) +kC\cos kd+kD\sin kd = 0 \quad (18)$$

Since the solution is valid for an interface that is almost parallel to the wall of the channel, θ can be taken to be approximately $\pi/2$. Substituting the corresponding values of $\psi(x, y)$ and θ into Eq. (12), the tangential stress boundary condition at the interface becomes

$$A(\cos k\lambda d - k\lambda d\sin k\lambda d - \tfrac{1}{2}\sin 2k\lambda d -\tfrac{1}{2}\cos 2k\lambda d\cos k\lambda d)+B\left(\sin k\lambda d+k\lambda d\cos k\lambda d +\tfrac{1}{2}\cos 2k\lambda d\sin k\lambda d-\tfrac{1}{2}\sin 2k\lambda d\cos k\lambda d\right) -2k^2C\cos k\lambda d-2k^2D\sin k\lambda d = 0 \quad \text{at } y=\lambda d-\varepsilon \quad (19)$$

As $\theta \to \pi$, $\varepsilon \to 0$, at the bubble surface ε can be neglected when compared with λd. Therefore, the radius of the bubble can be taken to be $y = \lambda d$ in Eq. (19).

The normal stress boundary condition at the interface is obtained in a similar manner. If Eqs. (15) and (16) are substituted into Eq. (13), the following expression is obtained:

$$\frac{k^2}{2C_a}\left(\frac{1}{(k\lambda d)^2}+1\right) +A\left(\frac{k\lambda d}{2}\cos k\lambda d+\frac{1}{4}\cos 2k\lambda d\sin k\lambda d -\frac{1}{4}\sin 2k\lambda d\cos k\lambda d\right) +B\left(\frac{k\lambda d}{2}\sin k\lambda d+\frac{1}{4}\sin 2k\lambda d\sin k\lambda d +\frac{1}{2}\cos 2k\lambda d\cos k\lambda d\right)-Ck^2\sin k\lambda d+Dk^2\cos k\lambda d = \frac{1}{2C_a}(p_0-F)\exp(-kx) = 0 \quad (20)$$

where p_0 is the pressure within the gas bubble and F an arbitrary constant which comes from the calculation of the viscous fluid pressure. Thus, F can be taken to be equal to

p_0 without loss of generality. The curvature of the interface are given by

$$\frac{1}{R} = \frac{d^2\varepsilon/\mathrm{d}x^2}{[1+(\mathrm{d}\varepsilon/\mathrm{d}x)^2]^{3/2}} + \frac{\varepsilon}{(\lambda d)^2}$$

for two-dimensional flow, and $(\mathrm{d}\varepsilon/\mathrm{d}x)^2 \ll 1$. If n_x and n_y are substituted into Eq. (11) and the resulted equation is rearranged by dividing by $\sin\theta$ and $\cot\theta$ is taken to be $\mathrm{d}\varepsilon/\mathrm{d}x$ which can be seen in Fig. 1, the kinematic boundary condition at the interface becomes

$$\frac{\mathrm{d}\varepsilon}{\mathrm{d}x} = \frac{\partial\psi}{\partial y}\frac{\mathrm{d}\varepsilon}{\mathrm{d}x} - \frac{\partial\psi}{\partial x}$$

On the right-hand side of the above equation the first term is negligible compared to the second term, and substituting for ψ and ε the above equation becomes

$$\begin{aligned}\varepsilon_0 \; &+A\left(\frac{\lambda d}{2k}\sin k\lambda d + \frac{1}{4k^2}\sin 2k\lambda d \sin k\lambda d\right.\\ &\left.+\frac{1}{4k^2}\cos 2k\lambda d\cos k\lambda d\right)\\ &+B\left(-\frac{\lambda d}{2k}\cos k\lambda d - \frac{1}{4k^2}\cos 2k\lambda d\sin k\lambda d\right.\\ &\left.+\frac{1}{4k^2}\sin 2k\lambda d\cos k\lambda d\right) + C\cos k\lambda d\\ &+D\sin k\lambda d = 0 \end{aligned} \tag{21}$$

Combining Eqs. (19) and (21) gives

$$k^2\varepsilon_0 + \tfrac{1}{2}A\cos k\lambda d + \tfrac{1}{2}B\sin k\lambda d = 0 \tag{22}$$

We now have five equations namely, Eqs. (17), (18) and (20)–(22) for a non-trivial solution. These five equations can be written in matrix form. After some of these equations are rearranged, the matrix form of the equations is given by

$$\begin{bmatrix} x_{11} & x_{12} & x_{13} & x_{14} & x_{15}\\ x_{21} & x_{22} & x_{23} & x_{24} & x_{25}\\ x_{31} & x_{32} & x_{33} & x_{34} & x_{35}\\ x_{41} & x_{42} & x_{43} & x_{44} & x_{45}\\ x_{51} & x_{52} & x_{53} & x_{54} & x_{55} \end{bmatrix}\begin{bmatrix} G_\mathrm{m}\\ A\\ B\\ C_\mathrm{m}\\ D_\mathrm{m}\end{bmatrix} = \begin{bmatrix}0\\0\\0\\0\\0\end{bmatrix} \tag{23}$$

where x_{ij} are

$$\begin{aligned}
&x_{11} = 1, \qquad x_{12} = \tfrac{1}{2}\cos k\lambda d, \qquad x_{13} = \tfrac{1}{2}\sin k\lambda d,\\
&x_{14} = 0, \qquad x_{15} = 0, \qquad x_{21} = 1,\\
&x_{22} = \tfrac{1}{2}k\lambda d\sin k\lambda d + \tfrac{1}{4}\sin 2k\lambda d\sin k\lambda d\\
&\qquad +\tfrac{1}{4}\cos 2k\lambda d\cos k\lambda d,\\
&x_{23} = -\tfrac{1}{2}k\lambda d\cos k\lambda d - \tfrac{1}{4}\cos 2k\lambda d\sin k\lambda d\\
&\qquad +\tfrac{1}{4}\sin 2k\lambda d\cos k\lambda d, \qquad x_{24} = \cos k\lambda d,\\
&x_{25} = \sin k\lambda d, \quad x_{31} = \frac{1}{2C_\mathrm{a}}[(k\lambda d)^{-2}+1],\\
&x_{32} = \tfrac{1}{2}k\lambda d\cos k\lambda d + \tfrac{1}{4}\cos 2k\lambda d\sin k\lambda d\\
&\qquad -\tfrac{1}{4}\sin 2k\lambda d\cos k\lambda d,\\
&x_{33} = \tfrac{1}{2}k\lambda d\sin k\lambda d + \tfrac{1}{4}\sin 2k\lambda d\sin k\lambda d\\
&\qquad +\tfrac{1}{4}\cos 2k\lambda d\cos k\lambda d,\\
&x_{34} = -\sin k\lambda d, \qquad x_{35} = \cos k\lambda d, \qquad x_{41} = 0,\\
&x_{42} = \tfrac{1}{2}kd\sin kd + \tfrac{1}{4}\sin 2kd\sin kd + \tfrac{1}{4}\cos 2kd\cos kd,\\
&x_{43} = -\tfrac{1}{2}kd\cos kd - \tfrac{1}{4}\cos 2kd\sin kd + \tfrac{1}{4}\sin 2kd\cos kd,\\
&x_{44} = \cos kd, \qquad x_{45} = \sin kd, \qquad x_{51} = 0,\\
&x_{52} = \tfrac{1}{2}\sin kd + \tfrac{1}{2}kd\cos kd + \tfrac{1}{4}\cos 2kd\sin kd\\
&\qquad -\tfrac{1}{4}\sin 2kd\cos kd,\\
&x_{53} = -\tfrac{1}{2}\cos kd + \tfrac{1}{2}kd\sin kd\\
&\qquad +\tfrac{1}{4}\sin 2kd\sin kd + \tfrac{1}{4}\cos 2kd\cos kd,\\
&x_{54} = -\sin kd, \qquad x_{55} = \cos kd
\end{aligned}$$

where G_m, C_m, and D_m are constants and are equal to $k^2\varepsilon_0$, k^2C, and k^2D, respectively. The first, fourth, and fifth columns of the matrix can be divided by k^2 in order to remove k^2 from Eq. (23) without changing the validity of the expression. The second term in Eq. (23) cannot be equal to zero. Therefore, the first term must be equal to zero.

In the gas-assisted displacement process, for two-dimensional flow, the relationships between the important quantities such as C_a, λ, and k are contained in Eq. (23) implicitly. These parameters determine the amount of liquid deposited on the walls of the channel. These quantities depend very much upon one another as shown in Fig. 2. The graphical relationship between C_a, λ, and kd (kd rather than k since all three quantities are non-dimensional) is drawn by keeping one of these three parameters constant, varying a second parameter and computing the third parameter.

4. Results and discussion

As mentioned previously, the relationship between the relevant governing parameters in gas-assisted displacement was obtained from this analysis implicitly. The analysis provides a satisfactory relationship between m and C_a for values of kd between 1.8 and 2.0. It is expected that the coating thickness obtained from this analysis for a rectangular channel is close to the experimental data for a value of kd taken to be 1.95 since the perturbation solution at low capillary number is close to this value of kd (see Fig. 2).

The eigenfunction solution, perturbation solution, and numerical solution have been compared with each other in Fig. 2 (for more detailed discussion, see [12]). It is found that the computed fraction of liquid deposited on the wall of a rectangular channel containing a Newtonian fluid determined from the eigenfunction solution is larger than that of the corresponding numerical solution.

The gas-assisted displacement of a Newtonian fluid in a circular tube was analyzed by Cox [1]. In his study, the experimental data are in close agreement with the theoretical analysis for $kd = 2$, where d is the tube radius. It was shown

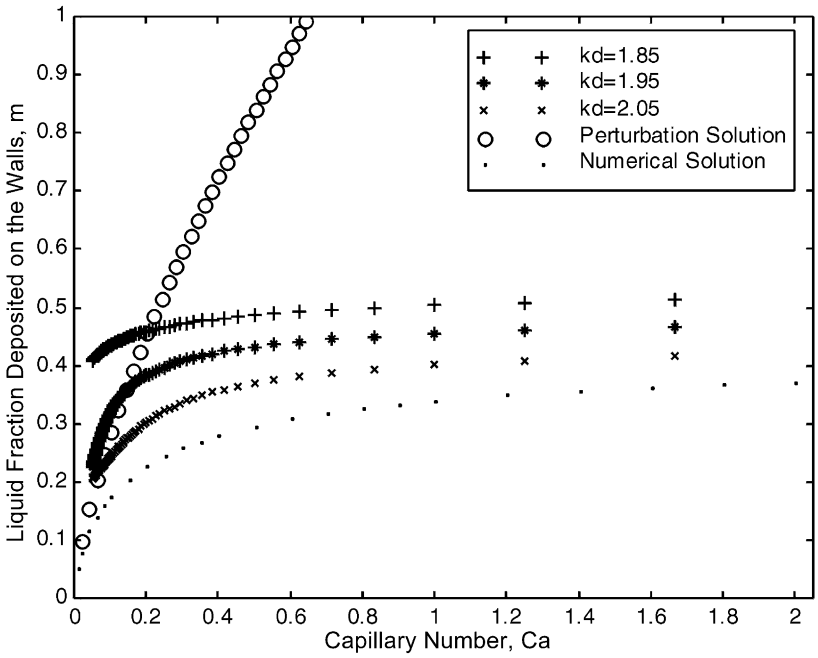

Fig. 2. Liquid fraction deposited on the walls of a rectangular channel as a function of capillary number for Newtonian fluids; eigenfunction solution $(+, *, x)$, perturbation solution $(\bigcirc)$, numerical results of Reinelt and Saffman $(\cdots)$.

that the solution is only valid under certain restrictions such as $\theta \to \pi/2$ and $kd = 2$.

In this analysis the solution is also valid for an gas–liquid interface is almost parallel to the walls of a rectangular channel and it was assumed that the tongue-like shape of the interface moved so slow that the fingering was not occurred. In other words, it is valid under the certain restriction such as $\theta \to \pi/2$ and for values of *kd* between 1.8 and 2.0. The fraction of Newtonian liquid deposited on the wall of a tube obtained from the approach presented here is almost identical to the experimental data for value of *kd* taken to be 2.0 [1]. On the other hand, in the case of a rectangular channel it is expected that the fractional coverage of a Newtonian fluid is close to the experimental data for value of *kd* taken to be 1.95 since, as stated previously, the perturbation solution at low capillary number is close to this value of *kd*.

The coating thickness obtained from the eigenfunction solution is larger than that obtained from the numerical solution. However, the numerical solution does not explicitly include values for *k* and *d*. Unfortunately, experimental data are not available for validating either the eigenfunction solution or the numerical solution and thus deciding which approach is more accurate. However, it is expected that the coating thickness obtained from this analysis for a rectangular channel is close to the experimental data for a value of *kd* taken to be 1.95 since the perturbation solution at low capillary number is close to this value of *kd* (see Fig. 2).

As can be seen in Fig. 2, the fraction of liquid deposited on the walls of a rectangular channel decreases with increasing values of *kd*. The computed liquid film thickness from the numerical analysis can be obtained by means of this analysis by varying the value of *kd*.

For different values of *kd*, the fraction of liquid deposited on the walls of a rectangular channel is shown as a function of capillary number for the case of a Newtonian fluid in Fig. 2. The perturbation analysis, eigenfunction solution, and the numerical data of Reinelt and Saffman [9] are also compared in Fig. 2. The perturbation solution is valid only for very small capillary numbers as evident in the figure. The eigenfunction solution is closer to the perturbation analysis than the numerical results of Reinelt and Saffman [9] for small capillary number as can be seen in Fig. 2.

5. Conclusions

This analysis provides a satisfactory relationship between m and C_a for values of *kd* between 1.8 and 2.0. Different values of *kd* result in various values of the liquid fraction deposited on the walls of a Hele-Shaw cell. It is expected that the coating thickness obtained from this analysis for a rectangular channel is close to the experimental data for a value of *kd* taken to be 1.95 since the perturbation solution at low capillary number is close to this value of *kd*.

References

[1] B.G. Cox, J. Fluid Mech. 14 (1962) 81.
[2] B.G. Cox, J. Fluid Mech. 20 (1964) 193.
[3] F.P. Bretherton, J. Fluid Mech. 10 (1961) 166.

[4] G.I. Taylor, J. Fluid Mech. 10 (1961) 161.
[5] C.W. Park, G.M. Homsy, J. Fluid Mech. 139 (1984) 291.
[6] J. Ratulowski, H.C. Chan, Phys. Fluids A 1 (1989) 1642.
[7] D.A. Reinelt, J. Fluid Mech. 183 (1987) 219.
[8] D.A. Reinelt, Phys. Fluids 30 (1987) 2617.
[9] D.A. Reinelt, P.G. Saffman, SIAM J. Sci. Statist. Comput. 6 (1985) 542.
[10] W.B. Kolb, R.L. Cerro, Phys. Fluids A 5 (1993) 1549.
[11] W.B. Kolb, R.L. Cerro, Chem. Eng. Sci. 46 (1991) 2181.
[12] F. Kamışlı, Mathematical analysis and experimental study of gas-assisted injection molding, Ph.D. Thesis, State University of New York at Buffalo, Buffalo, 1997.
[13] L.D. Landau, V.G. Levich, Acta Physicochim. URSS 17 (1942) 42.
[14] F. Fairbrother, A.E. Stubbs, J. Chem. Soc. 1 (1935) 527.
[15] L.W. Schwartz, H.W. Princen, A.D. Kiss, J. Fluid Mech. 172 (1986) 259.
[16] J.M. McLean, P.G. Saffman, J. Fluid Mech. 102 (1981) 455.
[17] T.S. Ro, G.M. Homsy, J. Non-Newt. Fluid Mech. 57 (1995) 203.
[18] E. Pitts, J. Fluid Mech. 97 (1980) 53.
[19] R.H. Marchessault, S.G. Mason, Ind. Eng. Chem. 52 (1960) 79.
[20] E.I. Shen, K.S. Udell, Trans. ASME E 52 (1985) 253.
[21] A.J. Poslinski, P.R. Oehler, V.K. Stokes, Polym. Eng. Sci. 35 (1995) 877.
[22] A.J. Poslinski, D.J. Coyle, Steady Gas Penetration through Non-Newtonian Liquids in Tube and Slit Geometries: Isothermal Shear-thinning Effects, Polymer Processing Society, 10th Annual Meeting, 1994.
[23] P. Tabeling, G. Zocchi, A. Libchaber, J. Fluid Mech. 177 (1987) 67.
[24] P.G. Saffman, G.I. Taylor, Proc. R. Soc. London A 245 (1958) 312.
[25] P.C. Huzyak, K.W. Koelling, J. Non-Newt. Fluid Mech. 71 (1997) 73.